

NPL REPORT MAT 76

EDGE CHIPPING OF CERAMIC CUTTING TOOLS

R Morrell, N J McCormick, and L A Lay

APRIL 2015

EDGE CHIPPING OF CERAMIC CUTTING TOOLS

R Morrell, N J McCormick and L A Lay
Materials Division

ABSTRACT

A reassessment of test data from experiments on the edge chipping of ceramic cutting tools has been made. These data were originally from an EU programme on development of novel nanocomposite ceramic cutting tools, and were obtained with the intention of forming a baseline data set against which to compare newly developed materials. In the light of further developments in the characterisation of edge chipping behaviour in ceramics, the data have been re-assessed with respect to test scatter, to the use of a blunt Rockwell indenter relative to sharp indentation, and to place the complete data set into the public domain.

© NPL Management Limited, 2015

ISSN 1754-2979

National Physical Laboratory
Hampton Road, Teddington, Middlesex, TW11 0LW

Extracts from this report may be reproduced provided the source is acknowledged
and the extract is not taken out of context.

Approved on behalf of NPLML by
Professor M G Gee, Science Leader, Materials Division

CONTENTS

1	INTRODUCTION	1
2	MATERIALS	1
3	TEST METHODS	2
3.1	EDGE-CHIP TESTS	2
3.2	OTHER INDENTATION TESTS	2
3.3	MICROSTRUCTURES	4
4	RESULTS	4
5	DISCUSSION	4
5.1	SCATTER IN TEST RESULTS	4
5.2	LINEARITY OF RELATIONSHIP	5
5.3	CORRELATION WITH CRACK RESISTANCE PARAMETERS	5
5.4	ANISOTROPIC MATERIALS	6
6	CONCLUSIONS	8
7	REFERENCES	9
	ANNEX: EDGE CHIPPING DATA PLOTS	11

(Intentionally blank)

1 INTRODUCTION

In 1992, NPL became involved with a European consortium targeting the development of novel nanocomposite ceramic cutting tool materials. Our role was one of characterising the microstructures and mechanical properties of new materials. One of the tests that was applied was the recently developed 'edge chipping' test in which a Rockwell indenter is driven into the material near an edge until a flake is formed and breaks away [1-4]. The force at which this occurs is recorded as a measure of the strength of the edge, which clearly has relevance to materials used as cutting tools for difficult-to-machine alloys, such as cast irons and nickel superalloys. With a Rockwell indenter, the force scales near-linearly with distance of the centre of indentation from the edge. The slope of the force/distance relationship has been termed 'edge toughness', T_e , having units of energy, $\text{N/m} = \text{J/m}^2$, which in principle can be correlated with other measures of material toughness, such as G_{Ic} or K_{Ic} .

In 1996, some of the data on cutting tools were presented at the *Pac-Rim 2 Ceramic Societies Conference* in Cairns, Australia, and published only electronically in the proceedings [5], unfortunately without the figures. Since then there have been numerous investigations of the edge chip process by other authors. Rather than using a spherically tipped Rockwell diamond, some authors have used different indenter forms, including Vickers pyramidal and conical geometries, both of which have consistent geometry relative to the distance from the edge, whereas the Rockwell indenter has a fixed tip radius of 0.2 mm. The force/distance from edge relationships vary significantly. For example Chai and Lawn [6] used a Vickers indenter with its diagonal axis aligned with the test-piece edge, and showed a force : (distance)^{3/2} relationship which they explained by conventional indentation fracture methodologies. Gogotsi *et al.* [7-10] have evaluated a number of materials in different ways and have made some proposals for universal relationships. Quinn *et al.* [11] have reviewed much data associated with dental materials, and find a variety of distance exponents when using different indenters. It is becoming clearer that the apparent force/distance from edge linearity achieved when using a Rockwell diamond indenter is a consequence, almost a quirk, of non-scaling indenter geometry relative to distance from edge, and that blunt indentation requires rather greater forces than sharp indentation to propagate the flake, probably because of a lesser wedging effect on penetration compared with sharp indentation. Quinn [12] has also provided a recent overview of all the research effort in the theme.

Following requests for more information on the statistical aspects of the edge chip process for standardisation purposes, this report has been prepared to place the earlier NPL work fully into the public domain as a formal record. There is a new evaluation of the scatter of data, and the fitting of functional dependences between force and distance from the edge.

2 MATERIALS

All the test materials were commercially acquired ceramic cutting tools in the form of typically 15 mm squares, with rounded corners, a small 20°-30° edge chamfer, and no central hole. Individual supplier codes are known, but not included here. Tool material types encompassed alumina, alumina/zirconia, silicon nitride, silicon nitride/titanium nitride and alumina/SiC whisker materials.

3 TEST METHODS

3.1 EDGE-CHIP TESTS

All the edge chip tests were made in an ET500¹ testing machine specifically designed for the purpose. Polycrystalline diamond Rockwell indenters of standard 0.2 mm tip radius were used throughout. The edge of the test-piece could be sighted through a microscope, the cross-wires of which were aligned with the indenter axis. The microscope could then be withdrawn to be replaced with the indenter, and the X-Y stage then moved to the appropriate distance from the edge using the digital positioning readout. The test force was then applied to the indenter until the flake was produced. In all cases the flake production correlated with a load drop, the detection of which permitted immediate off-loading and peak load recording.

Indentations were made at pre-determined distances from the edge by loading at 0.5 mm/min displacement rate. The load-drop detection system of the machine unloaded the indenter once a flake was formed. This process was performed many times on all eight edges of the cutting tools, making sure that there was no overlap of the flakes. Up to 30 flakes were produced on each type of cutting tool, typically half of which were at a given distance from the edge (usually at about 0.4 mm) and the remainder over the range 0.2 to 1.0 mm. The minimum distance from the edge was governed by the size of the edge chamfer, but was typically 0.25 mm. The maximum distance was governed by the tool thickness, but was typically 1.0 to 1.2 mm. In order to ascertain the statistical nature of the process, generally more than 10 chips were made at the same distance from the edge.

3.2 OTHER INDENTATION TESTS

Because of the small size of the test-pieces which makes normal plane strain fracture toughness testing somewhat difficult to undertake, in order to complement the edge chipping tests, indentation tests were made on polished test-piece surfaces using HV5 indentations, and the hardness measured. In addition, the crack lengths emanating from the indentation corners were also measured. Because it was unclear what the geometrical nature of the induced cracking was in the range of test materials, in order to evaluate these data, two approaches were taken.

The first was to employ the route taken for cemented carbides and hardmetals, assuming that the cracks were of a Palmqvist, near-surface type [13, 14, 15, 16]. The so-called Palmqvist crack resistance, derived from the experimentally derived linear relationship between crack length and force, is given by $R_1 = P/b$ (in N/m), where P is the indentation force and b is the total crack length of all four cracks from the indentation corners. Palmqvist toughness (in MN/m^{3/2}) is given by $R_2 = 0.0028(HR_1)^{1/2}$ where H is the hardness in N/mm² (or alternatively $R_2 = 0.0889(HR_1)^{1/2}$ with H in GPa [16]), although as noted by [15], it is largely empirical, and does not represent behaviour at high toughness levels.

The second approach was to employ the indentation fracture mechanics for ceramics based on the assumption of half-penny shaped cracks. Two equations were employed, that of Miyoshi [17]:

$$K_{R1} = 0.0264 E^{0.5} P^{0.5} c^{-1.5} a$$

and that of Marshall and Evans [18]:

$$K_{R2} = 0.036 E^{0.4} P^{0.6} c^{-1.5} a^{0.8}$$

where in both cases E is Young's modulus, c is the Vickers halfpenny crack radius, and a is the indentation half diagonal. It is recognised that these expressions are for quasistatic crack resistance parameters, and not true fracture toughness, as fully explored by Bradt and Quinn [19], but since the edge chipping process is related to indentation cracking, in fact the basis for its initiation, it remains relevant to employ the technique to make a comparison with edge-chipping behaviour. Since this work

¹ Engineering Systems, Nottingham, Ltd.

Table 1 – Materials and summary of experimental results

Material no.	Type	Edge toughness, T_e , N mm^{-1}			Hardness, HV5	Palmqvist total crack length, b , μm	Palmqvist parameters			Vickers parameters	
		Average at 0.42 mm	Unforced linear fit	Linear fit forced to zero			R_1 , N mm^{-1}	R_2 , $\text{MPa m}^{1/2}$	G_c , J m^{-2}	K_{R1} , $\text{MPa m}^{1/2}$	K_{R2} , $\text{MPa m}^{1/2}$
1	Al_2O_3	602 ± 50	656	596	1771 ± 89	257 ± 16	191	5.1	67	4.1	4.4
2	$\text{Al}_2\text{O}_3/\text{ZrO}_2$	693 ± 40	668	687	1690 ± 39	213 ± 34	230	5.5	77	4.9	5.2
3	$\text{Al}_2\text{O}_3/\text{ZrO}_2$	745 ± 71	698	715	1664 ± 44	199 ± 23	246	5.6	85	5.2	5.6
4	$\text{Al}_2\text{O}_3/\text{ZrO}_2$	683 ± 50	724	685	1717 ± 39	257 ± 22	191	5.0	65	4.2	4.5
5	$\text{Al}_2\text{O}_3/\text{ZrO}_2$	688 ± 62	670	677	1694 ± 39	237 ± 24	207	5.2	69	4.5	4.9
6	$\text{Al}_2\text{O}_3/\text{TiC}$	707 ± 40	738	712	2041 ± 60	211 ± 9	232	6.0	83	5.1	5.5
7	$\text{Al}_2\text{O}_3/\text{TiC}$	730 ± 55	699	707	1884 ± 41	176 ± 34	278	6.4	92	6.1	6.6
8	$\text{Al}_2\text{O}_3/\text{TiC}$	458 ± 29	477	470	2140 ± 60	182 ± 35	269	6.7	101	6.1	6.3
9	$\text{Al}_2\text{O}_3/\text{SiC}_w$	1083 ± 120	1061	1073	2087 ± 54	130 ± 18	377	7.8	146	7.4	8.1
10	$\text{Al}_2\text{O}_3/\text{SiC}_w$	827 ± 58	802	818	1967 ± 29	164 ± 22	299	6.7	109	6.3	6.8
11	$\text{Al}_2\text{O}_3/\text{SiC}_w$	1194 ± 177	Indented perpendicular to hot-pressing plane								
		987 ± 114	Indented parallel to hot-pressing plane								
12	Si_3N_4	632 ± 80	636	622	1394 ± 46	123 ± 27	399	6.5	148	6.7	7.3
13	Si_3N_4	622 ± 42	680	645	1675 ± 39	166 ± 22	290	6.1	133	5.1	5.7
14	Si_3N_4	879 ± 80	941	897	1591 ± 21	138 ± 17	355	6.6	161	5.9	6.6
15	Si_3N_4	811 ± 46	963	846	1465 ± 32	147 ± 8	333	6.1	129	5.9	6.5
16	Si_3N_4	555 ± 44	773	631	1617 ± 55	140 ± 9	350	6.6	155	6.0	6.6
17	$\text{Si}_3\text{N}_4/\text{TiN}$	734 ± 51	847	773	1454 ± 65	83 ± 32	591	8.1	194	9.1	9.7

was undertaken, a new ISO standard for indentation fracture resistance has been produced [20]², which could in principle be used for any situations where the test-piece size can be very small.

3.3 MICROSTRUCTURES

Microstructures were determined by polishing and etching the test-pieces, with SEM examination. Oxide materials were thermally etched at as low a temperature as was sufficient to produce grain boundary grooving visible in the SEM in order to minimise the risk of grain growth. Silicon nitride materials were plasma etched using CF₄ in O₂ [22].

4 RESULTS

Plots were prepared of the edge chipping force versus distance from the edge (DFE) for each tool type (see Annex), excluding material 11. The edge toughness was computed as the average value determined from the 10 or more chips made at the same distance from the edge, and by a linear fit to all data for all distances from the edge. There was no evidence of curvature in the plots outside the scatter band of the data that justified a higher power fit. In order to address the question of whether there is a zero offset, the linear fits were made without and with force-fitting through zero.

Table 1 summarises all the results. Three values of edge toughness are shown for comparison. All have the same units, but are obtained by different analyses. The first is the force/distance at a prescribed distance (0.42 mm) from the edge. The second two are the slopes of the best fitted line, with either the best linear fit, or the best linear fit with the intercept forced through zero. It can be seen that the edge chip resistance varies significantly among the various cutting tool types. In the main, the results determined by the zero-forced linear fit are within the standard deviation about the mean value determined at 0.40 or 0.42 mm distance from edge. The unforced fits sometimes lie outside the standard deviation, but such fits tend to be strongly biased by a single data point at the larger distances from edge. Table 1 also shows the data from the Vickers indentation testing to measure hardness and the length of the radial cracks from the indent corners, together with estimates of indentation fracture resistance using the Miyoshi and Evans/Marshall equations.

5 DISCUSSION

5.1 SCATTER IN TEST RESULTS

As the force is increased during indentation, radial cracks are developed which propagate ahead of the contact region between the indenter tip and the test material. The positions of crack initiation are presumably random, but the proximity of the indenter to the edge of the test-piece means that the hoop stress around the indenter, as determined from a pressurised pipe model [3], is not uniform but has maxima at typically $\pm 70^\circ$ to the edge normal. (It has been shown that in fact these positions are represented by tangents to the circle of contact of lines with an origin at the edge [3].) This causes cracks initiated in these regions to propagate in preference to those at other orientations (except when very close to the edge), and results in the classic shape of flake which is always thickest at the point of indentation. However, since the initiation of fracture under the indenter is a random process, the initiation angles are not unique, and this leads to some shape variation, notably some asymmetry.

²The standard, which is specifically for silicon nitride bearing balls, refers to a method attributable to Niihara, but does not cite a reference for the equation which is parametrically identical to the Marshall/Evans equation [18]:

$$K_{IFR} = 0.000978 \left(\frac{E}{H} \right)^{0.4} \left(\frac{P}{c^{1.5}} \right)$$

with E and H in GPa, P in N, and c in mm, giving K_{IFR} in MPa m^{1/2}. It is believed that the source is [21], assuming the 'constraint factor' cited is exactly 3. This equation gives an outcome 16.8% greater than the Marshall/Evans equation. It is also noted in the text of the standard, referencing [22], that if silicon nitrides are indented at >98 N force the cracks are of half-penny shape, not Palmqvist. This is twice the force level used in our original work.

While it is not clear whether asymmetry correlates strongly with flaking load, there is certainly some variation in flaking load, even in cutting tool materials which have very fine grained and uniform, pore-free microstructures. The coefficient of variation was found to be typically 0.05 to 0.1, somewhat less than the scatter normally determined in strength tests. This is because, unlike strength testing, the result is not influenced significantly by pre-existing surface flaws or isolated defects. The ability of this test to discriminate between materials is thus rather better than that experienced in conventional strength testing.

5.2 LINEARITY OF RELATIONSHIP

In normal sharp contact indentation fracture, the crack length c produced under a given indentation force P is normally given by a relationship of the type $P \propto c^{1.5}$, assuming that hardness and toughness are size scale independent. In the current situation the linear relationship between P and c has been clearly demonstrated over a large range in d , the distance from the edge, showing that normal sharp indentation mechanics are inappropriate. Consideration has to be given to the perturbation that the free side surface makes to the stress field into which the main flaking crack is being driven. It is thought that the hoop tensile stresses which cause the crack to propagate will decline with distance from the indentation site, but the edge perturbation causes the stress field to level off or even increase as the edge is approached. Thus a crack, which would normally grow stably, will accelerate as it approaches the edge, and the position at which this acceleration takes place is defined solely by geometry, not by load or elastic characteristics of the test material. This means that on indenting a given distance from the edge, the instability position will be the same for all materials, independent of toughness. However, the force required to drive the crack to this position depends on toughness, and it is this relationship which explains the existence of a 'master curve' for all materials [3, 4]. However, this does not explain the demonstrated linearity of load/distance from edge relationship, which is in contrast to normal sharp indentation fracture. In the absence of a good mathematical analysis, this remains unclear, but may be associated with the mixed mode stressing thought to occur as a result of the partition of the indenting force between the developing flake and the bulk of the material, *i.e.* on the two sides of the major flaking crack. This is effectively absent from long cracks in normal symmetrically loaded indentation mechanics. In the present case, the shear mode stress intensity factor would be essentially independent of the length of the crack, while the opening mode is a function of crack length at a given applied force. The dependence of size is thus likely to be less than the power of 1.5 normally seen.

5.3 CORRELATION WITH CRACK RESISTANCE PARAMETERS

Because of the small size of cutting tools, there is little practical alternative to indentation methods for determining indentation fracture resistance as a measure of toughness. Table 1 gives the results of HV5 indentation tests measuring the crack length and indentation size made on polished cross-section of the test materials. At least six indentations with well-formed measurable cracks were employed. Because it is not always clear whether the indentation crack is of Vickers half-penny or Palmqvist surface type, or somewhere between, the results were analysed for both cases and compared. In all cases, Young's modulus E was estimated from literature data for near fully dense materials of similar microstructures. The choice of these analysis methods was arbitrary, but followed those employed in a contemporary VAMAS round robin on toughness measurement [23].

Figure 1 shows examples of attempted correlations between the slopes of the indentation versus distance from edge lines (*i.e.* 'edge toughness', T_e , determined using the 0.42 mm from edge data) and the indentation crack resistance, K_R , calculated by the above methods. The solid lines show a lower boundary to the 'edge toughness' trend, with most datapoints lying to the left of this line. The correlation band is reasonable for all but five materials, nos. 12, 13, and 16, which are all silicon nitrides with elongated grains perhaps 5 μm in length, and no. 17, which is reinforced with $>3 \mu\text{m}$ TiN particles but the Si_3N_4 grain size is sub-micrometre. One alumina/TiC material (no.7) is also well away from any distinct trend. In these materials, the 'edge toughness' determined is low compared with what might have been expected from the general trend of indentation fracture resistance in the other

materials. In contrast, three other silicon nitride based materials with similar microstructures followed the general correlation. The reasons for this behaviour are unclear, but may be associated with whether the true indentation crack behaviour at 49 N indentation force is of Palmqvist or Vickers half-penny type, and if the former, the extent to which the result is influenced by the means of test-piece preparation. Further, the edge chipping data could be determined by factors such as residual surface stress from machining, or grinding damage. However, it is clear that of the two types of test, the edge toughness test seems to be a more pragmatic measure of resistance to edge fracture than an indentation test. These results provide further evidence that ‘edge toughness’ is indeed related to more-conventional methods of measuring toughness, even though the exact nature of the fracture mode is unclear.

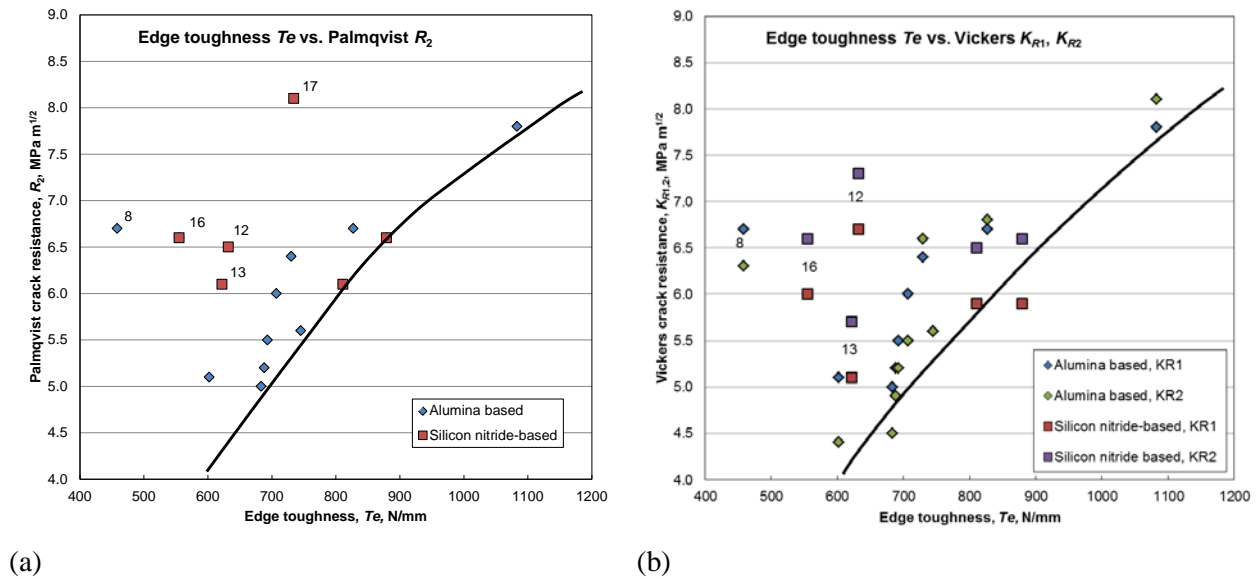


Figure 1: Correlations between ‘edge toughness’ and indentation fracture resistance for (a) Palmqvist and (b) Vickers analyses, using an indentation distance of 0.42 mm from the edge.

5.4 ANISOTROPIC MATERIALS

Previous work showed that single-crystal sapphire displays different behaviours when edge-flaked on orthogonal crystallographic orientations, while PMMA showed results which were not entirely self-consistent [3]. The reason was considered to be that the elasticity of these materials is anisotropic, and this controls the stress field developed under edge loading, modifying the edge toughness and the flake shape. In the present work, it has been found that material 11, which is hot-pressed alumina with SiC whiskers, also shows anisotropic behaviour (Table 1). This is fully in accordance with expectations that when tested such that the edge crack has to run principally across the plane of reinforcing whiskers, a higher toughness is recorded than when the crack is running mainly parallel to the reinforcing whiskers. In addition, the flake shape is modified. When indented perpendicular to the whisker plane, the crack tends to turn sharply towards the free surface giving a flake which is shallow compared with its width, whereas in the orthogonal direction, the flake is deeper and with a sharper edge. The test is therefore a useful means of identifying anisotropy. A typical microstructure of such a material is shown in Figure 2.

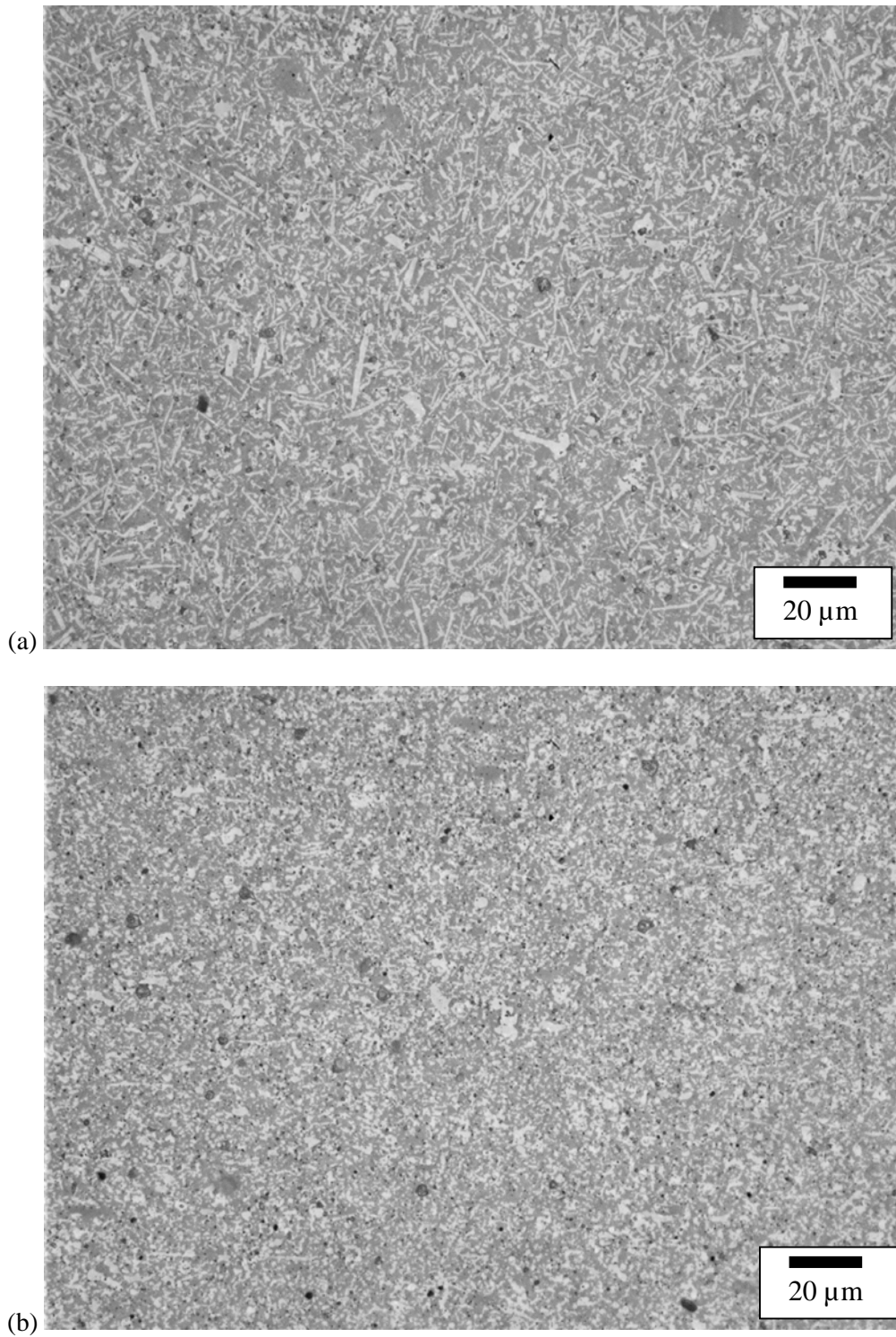


Figure 2: Microstructural anisotropy in a 15 mm square alumina/SiC_w cutting tool, (a) in the plane of the tool, and (b) in a transverse section with the plane of the tool horizontal.

6 CONCLUSIONS

A variety of commercially available cutting tools have been subjected to an edge chipping test by indenting near to a free edge with a Rockwell diamond indenter. It has been shown that:

1. The Rockwell indenter geometry results in an approximately linear relationship between chipping force and distance of the centre of indentation from the edge. There was no evidence of significant departure from linearity requiring a power law fit, as suggested by some other authors. The linearity is probably a consequence of the non-scaling geometry of a fixed radius Rockwell diamond tip, compared with self-scaling of Vickers, conical or Berkovitch sharp indenters.
2. At a fixed distance from the edge, the repeatability of result is shown as a coefficient of variation of 5%-10%. 'Edge toughness', T_e , defined as chipping force divided by distance from the edge, is in the range 450 to 1200 N m⁻¹.
3. Correlations have been made between 'edge toughness' and indentation fracture resistance determined as the radial crack lengths emanating from a sharp indentation remote from the test-piece edge, and employing both Palmqvist surface crack and Vickers half-penny crack analyses. Oxide and oxide composite materials show reasonable correlations, but silicon nitrides and non-oxide composites generally depart from such a correlation. The reasons for this are unclear.
4. Microstructurally anisotropic materials have been shown to have anisotropic 'edge toughness', with an alumina/SiC_w cutting tool being a clear example
5. The edge chipping test distinguishes between materials of different microstructures and resistances to edge damage.

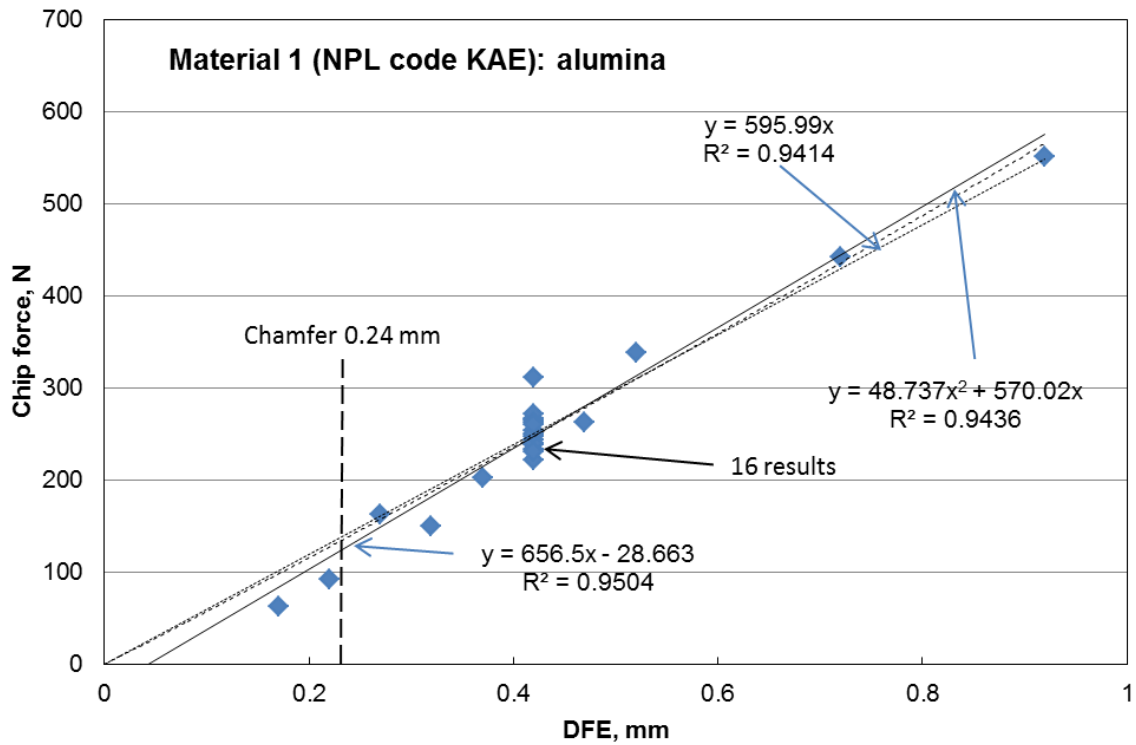
7 REFERENCES

1. McCormick, N.J., Almond, E.A. Constant-geometry edge-flaking of brittle materials. *Nature*, 1986, **321**(6065), 53-5.
2. McCormick, N.J. Edge flaking of brittle materials. *Proc. Brit. Ceram. Soc.*, 1990, **46**, 307-18.
3. McCormick, N.J. Edge flaking of brittle materials. *J. Hard. Materials*, 1990, **1**(1), 25-51.
4. McCormick, N.J. Edge flaking as a measure of material performance. *Metals and Materials*, 1992, (3), 154-6.
5. Morrell, R., McCormick, N.J. Edge chipping as an indicator of toughness. *Pac-Rim 2 Ceramic Societies Conference, Cairns, Australia, 15-17 July 1996*, in the Proceedings CD, 1998, Session 25C, Paper 816.
6. Chai, H., Lawn, B.R. A universal relation for edge chipping from sharp contacts in brittle materials: A simple means of toughness evaluation. *Acta Met.*, 2005, **55**(7), 2555-2561.
7. Gogotsi, G., Mudrik, S., Rendtel, A. Sensitivity of silicon carbide and other ceramics to edge fracture: method and results, *Cer. Eng. Sci. Proc.*, 2004, **25**(4), 237-246.
8. Gogotsi, G., Mudrik, S., Galenko, V. Evaluation of fracture resistance of ceramics: edge fracture tests, *Ceram. Int.*, 2007, **33**, 315-320.
9. Gogotsi, G., Mudrik, S. Fracture barrier estimation by the edge fracture test method, *Ceram. Int.*, 2009, **35**, 1871- 1875.
10. Gogotsi, G., Galenko, V. I., Mudrik, S.P., Ozersky, B.I., Khvorostyany, V.V., Khristevich, T. A. Fracture behavior of Y-TZP ceramics: new outcomes, *Ceram. Int.*, 2010, **36**, 345-350.
11. Quinn, J.B., Quinn, G.D., Hoffmann, K.M. Edge chip fracture resistance of dental materials. *Ceram. Eng. Sci. Proc.*, 2012, **33**(2), 71-84.
12. Quinn, G.D., Edge chip testing of ceramics. *Bull Amer. Ceram. Soc.*, 2012, **92**(1), 24-28.
13. Exner, H.E. The influence of sample preparation on Palmqvist's method for toughness testing of cemented carbides. *Trans. TMS-AIME*, 1969, 245, 677-83.
14. Viswanadham, R.K., Venables, J.D. A simple method for evaluating cemented carbides. *Met. Trans.*, 1977, **8A**, 187-191.
15. Warren, R., Maztke, H.J. Indentation testing of a broad range of cemented carbides. *Proc. 1st Int. Conf. on Science of Hard Materials, 1980*, edited by Viswanadham, Rowcliffe Gurland, Plenum Press, New York, 1981, pp 563-582.
16. Shetty, D.K., Wright, I.G., Mincer, P.N., Clauer, A.H. Indentation fracture of WC-Co cermets. *J. Mater. Sci.*, 1985, **20**, 1873-1882.
17. Miyoshi, T., Sagawa, N., Sassa, T. Study on fracture toughness evaluation for structural ceramics. *Proc JSME*, 1985, **A51**(471), 2487-89.
18. Marshall, D.B., Evans, A.G. Reply to "Comment on 'Elastic/Plastic Indentation Damage in Ceramics: The Median/ Radial Crack System'" . *J. Amer. Ceram. Soc.*, 1981, **64**(12), C-182-C-183.
19. Bradt, R.C., Quinn, G.D. On the Vickers indentation fracture toughness test. *J. Amer. Ceram. Soc.*, 2007, 90 (3), 673-680.
20. ISO 14627: 2012 Fine ceramics (advanced ceramics, advanced technical ceramics) - Test method for fracture resistance of silicon nitride materials for rolling bearing balls at room temperature.
21. Niihara, K., Morena, R., Hasselman, D.P.H. Evaluation of K_{Ic} of brittle solids by the indentation method with low crack-to-indent ratios. *J. Mater. Sci. Lett.*, 1982, **1**(1), 13-16.

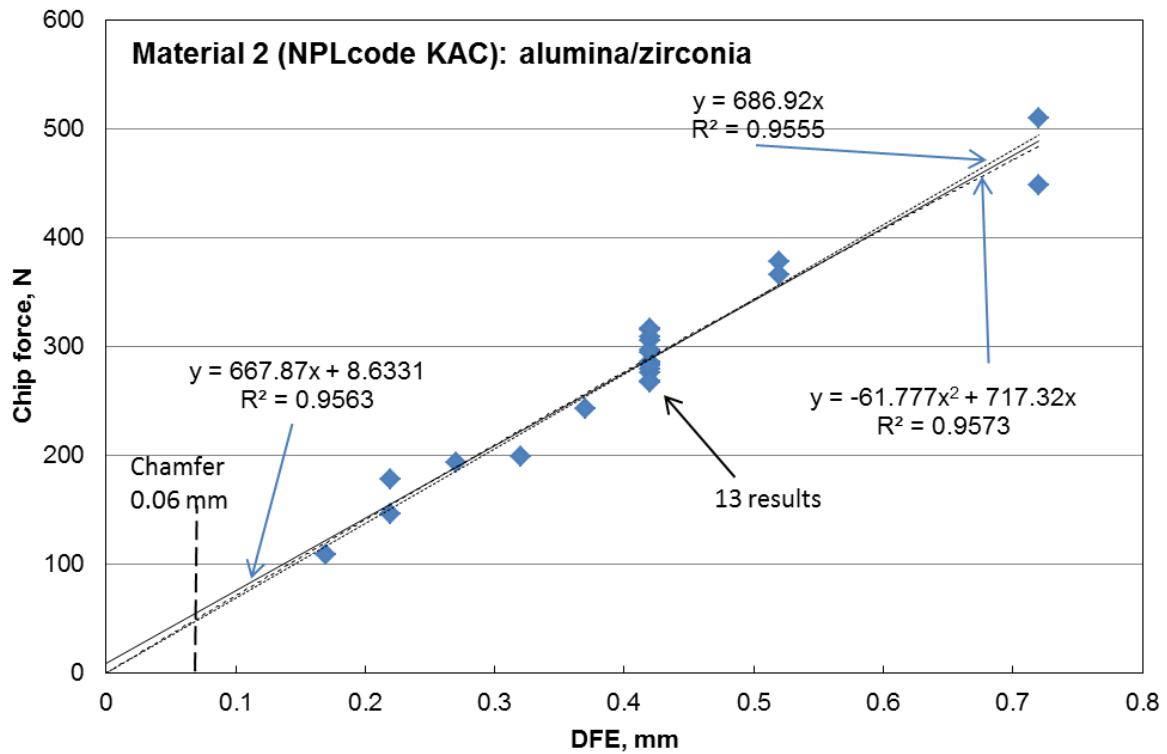
22. Miyazaki, H., Hyuga, H., Yoshizawa, Y., Hirao, K., Ohji, T. Crack profiles under a Vickers indentation in silicon nitride ceramics with various microstructures. *Ceram. Int.*, 2010, **36**, 173-9.
23. Chatfield, C., Norström, M., Plasma etching of sialon. *J. Amer. Ceram. Soc.*, 1983, **64**(9), C168.
24. Awaji, H., Kon, J.-I., Okuda, H. The VAMAS fracture toughness test round robin. VAMAS Technical report No. 9, 1990, 52pp.

ANNEX: EDGE CHIPPING DATA PLOTS

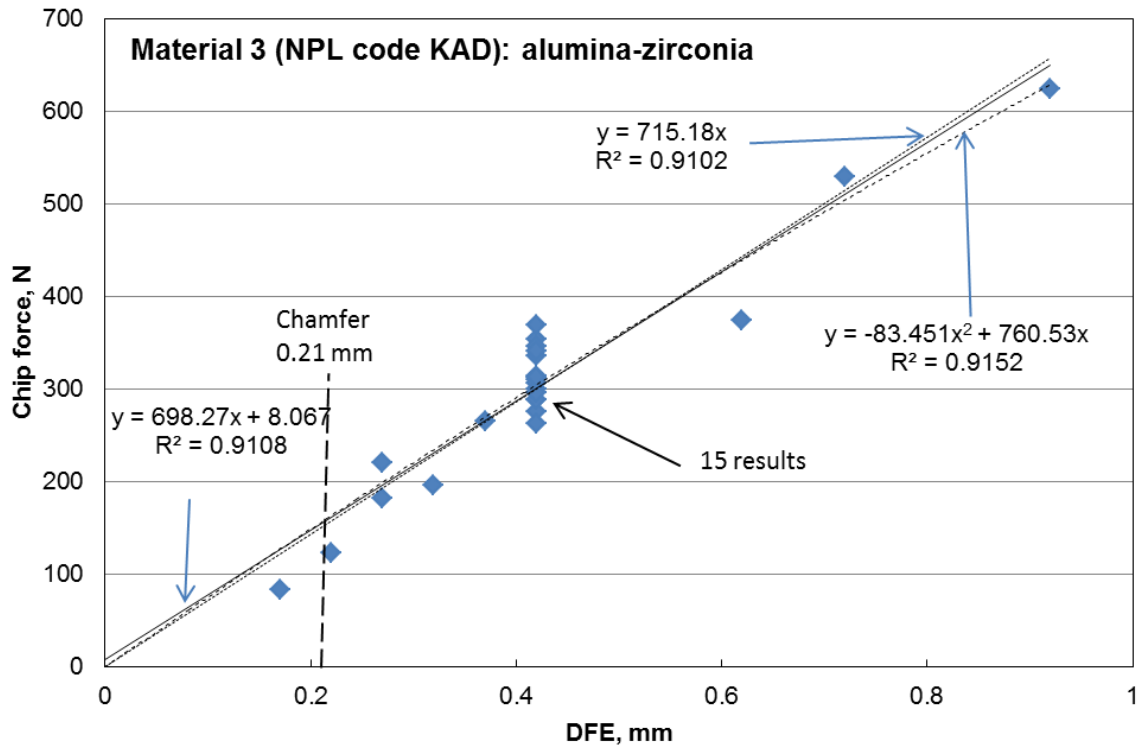
Material 1. Alumina



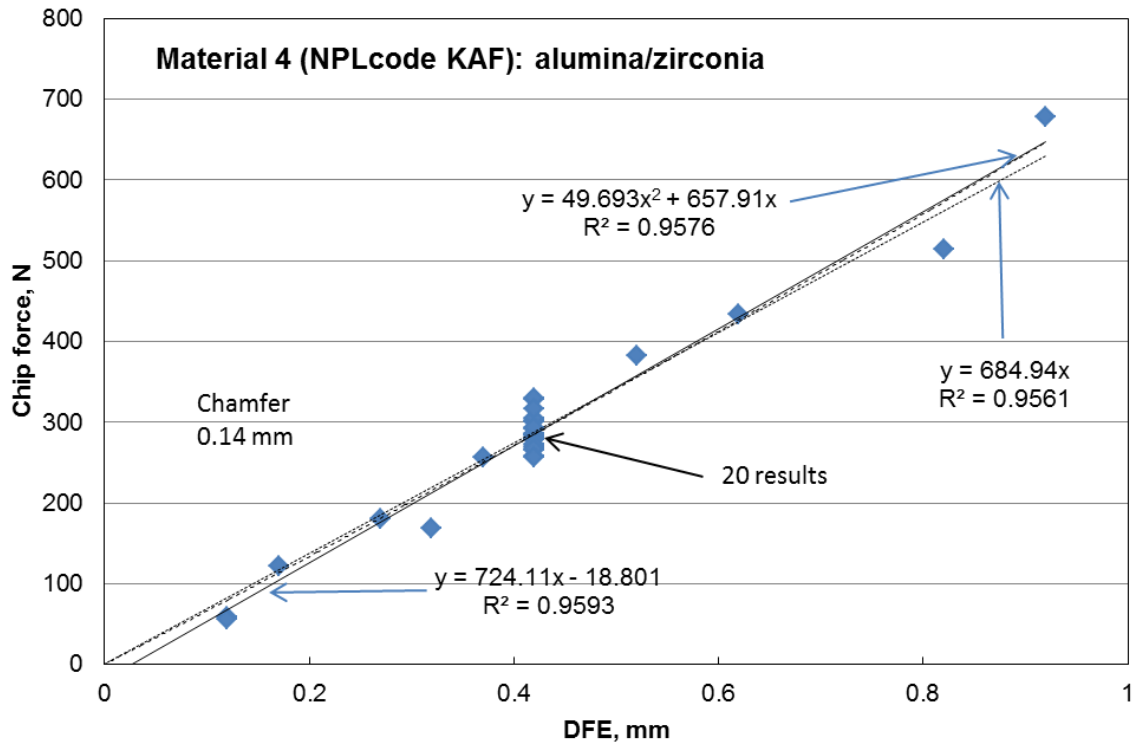
Material 2. Alumina/zirconia



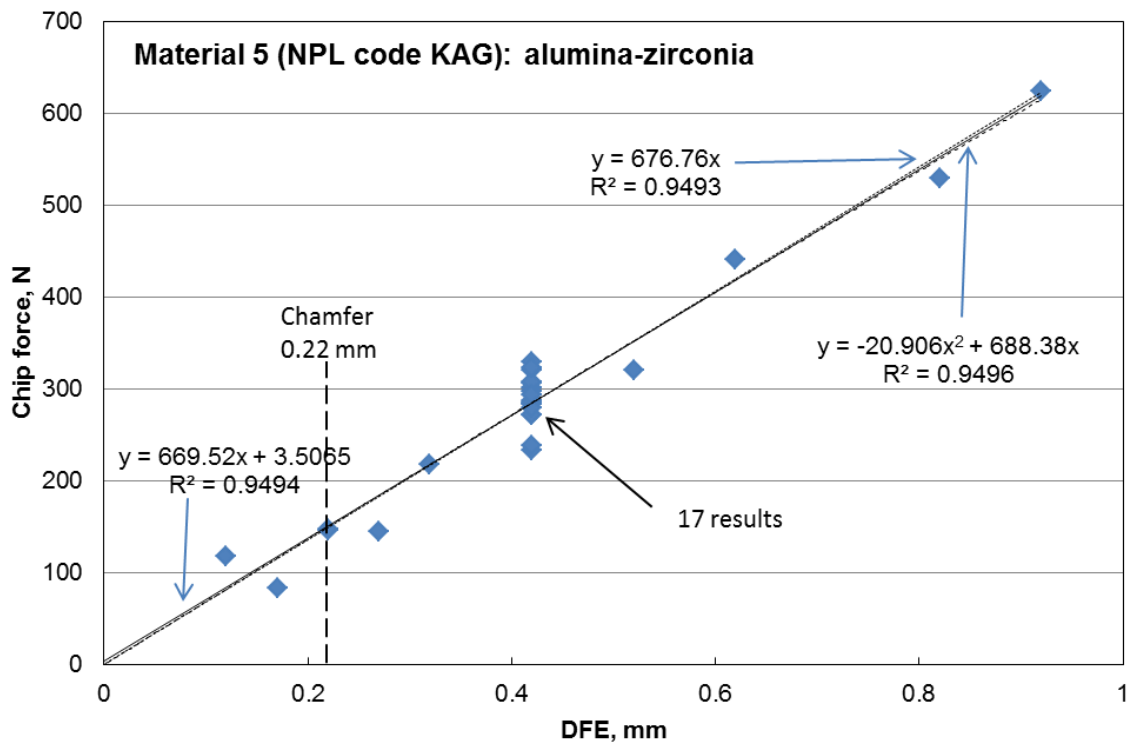
Material 3. Alumina/zirconia



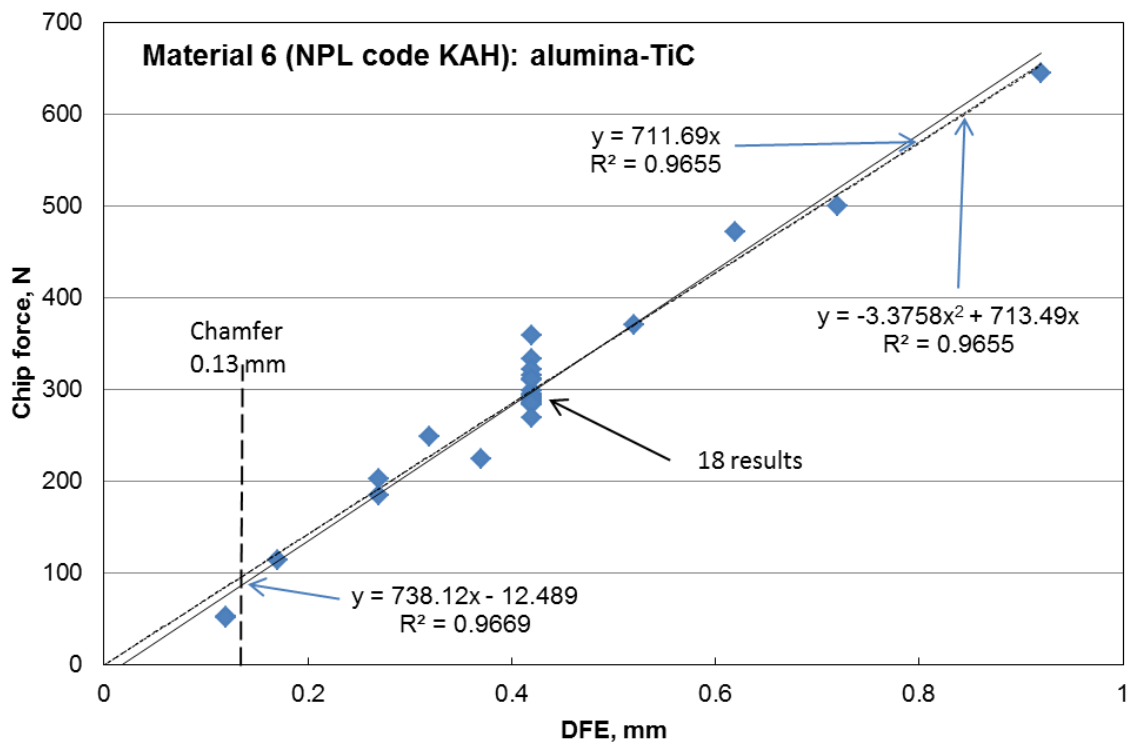
Material 4. Alumina/zirconia



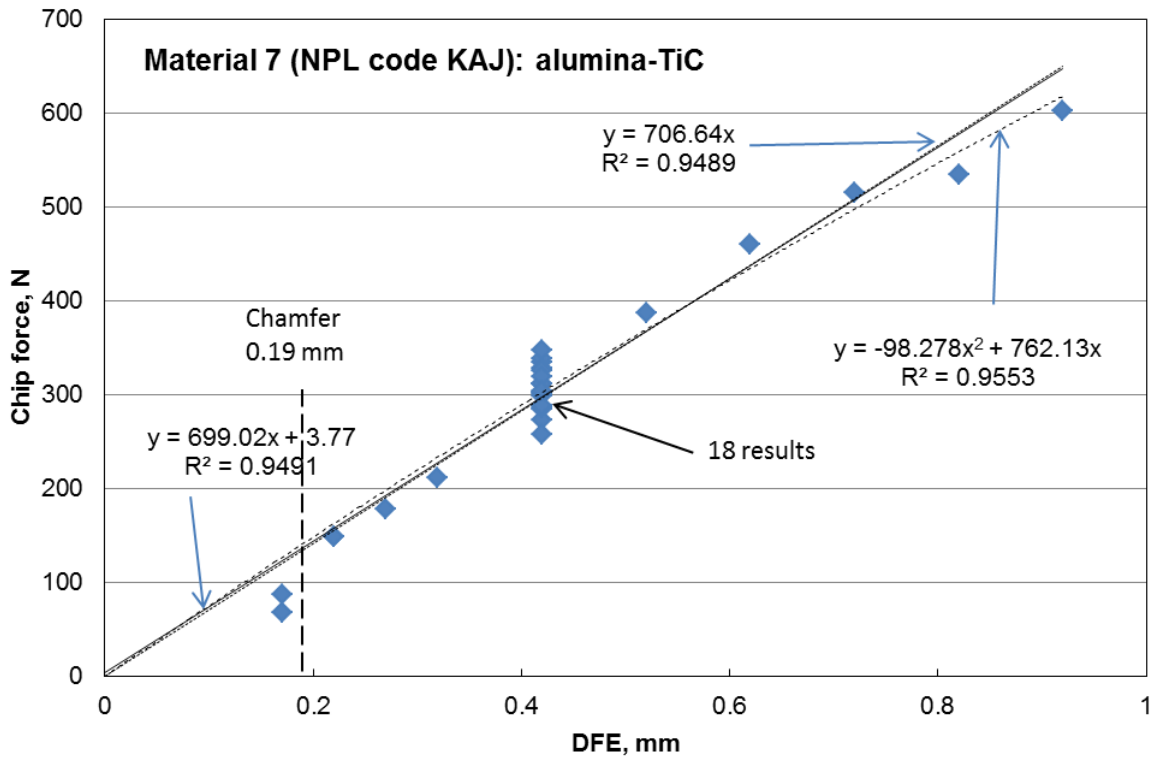
Material 5. Alumina/zirconia



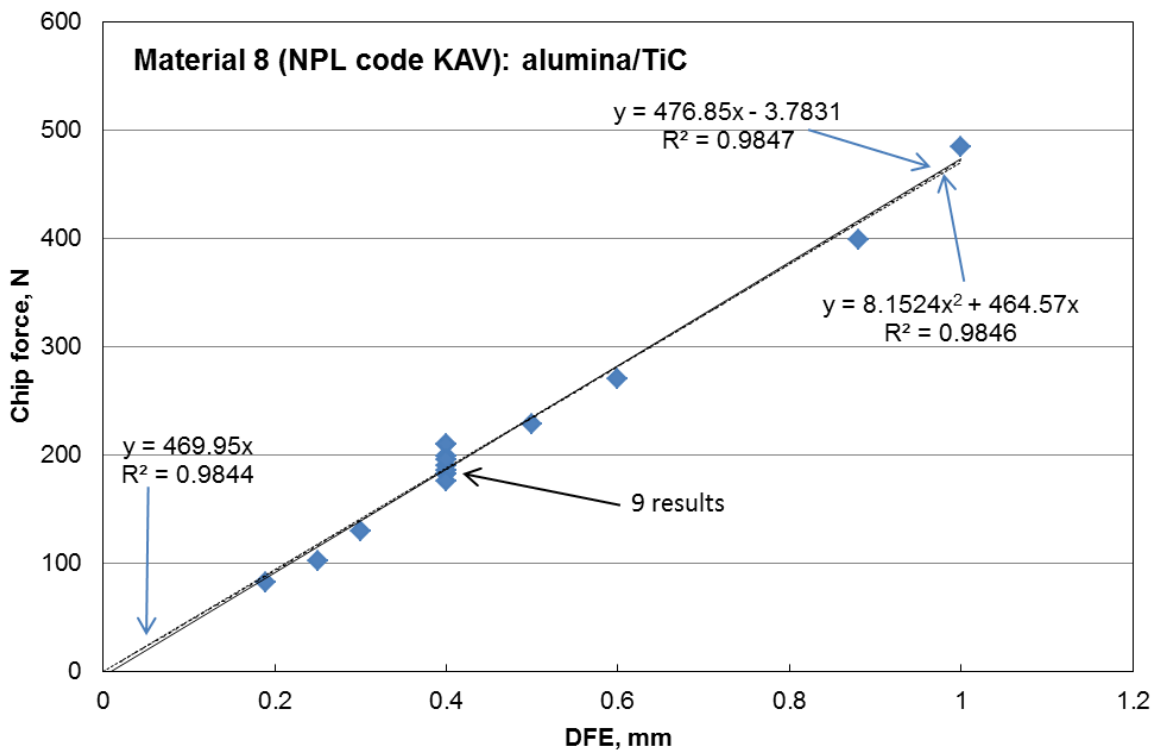
Material 6. Alumina/zirconia



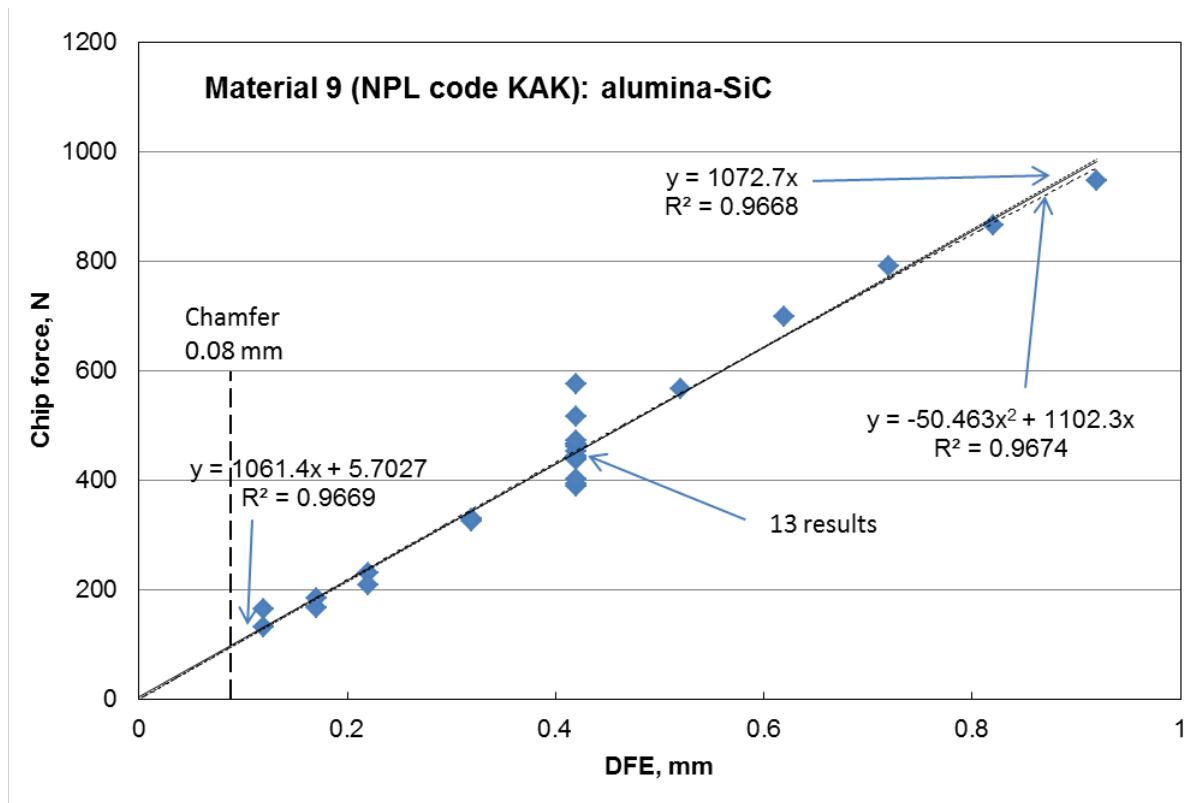
Material 7. Alumina/titanium carbide



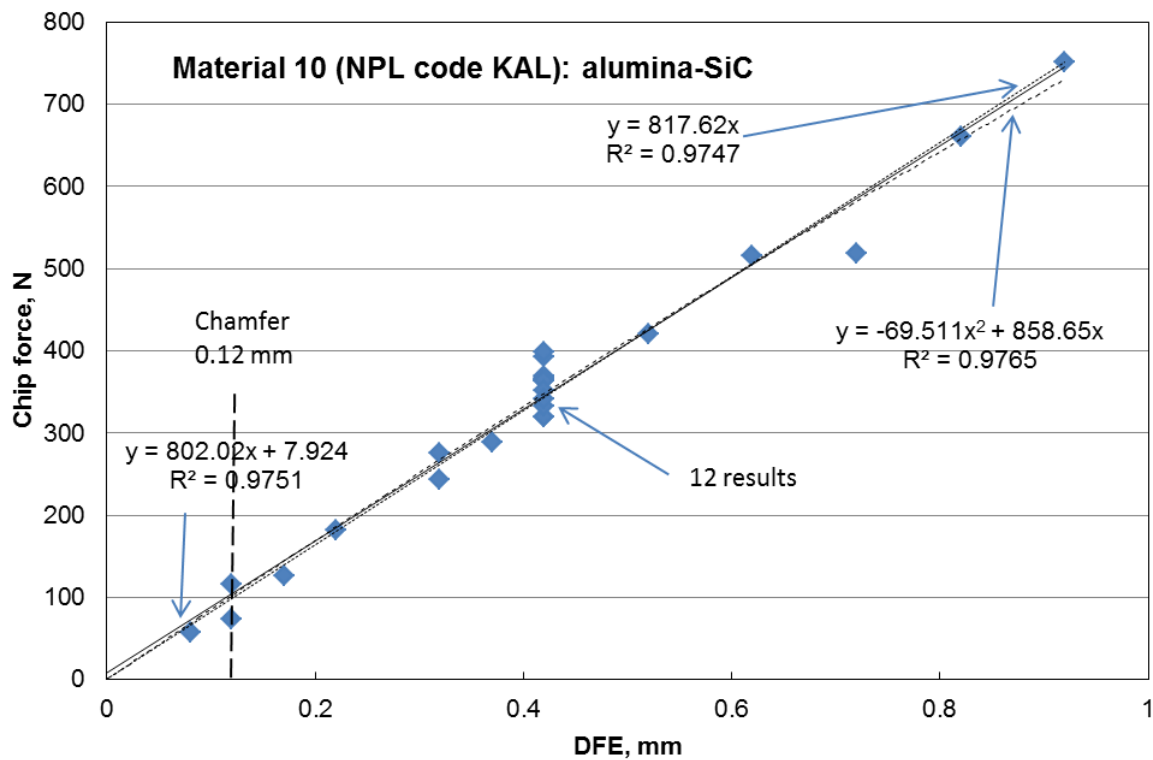
Material 8. Alumina/titanium carbide



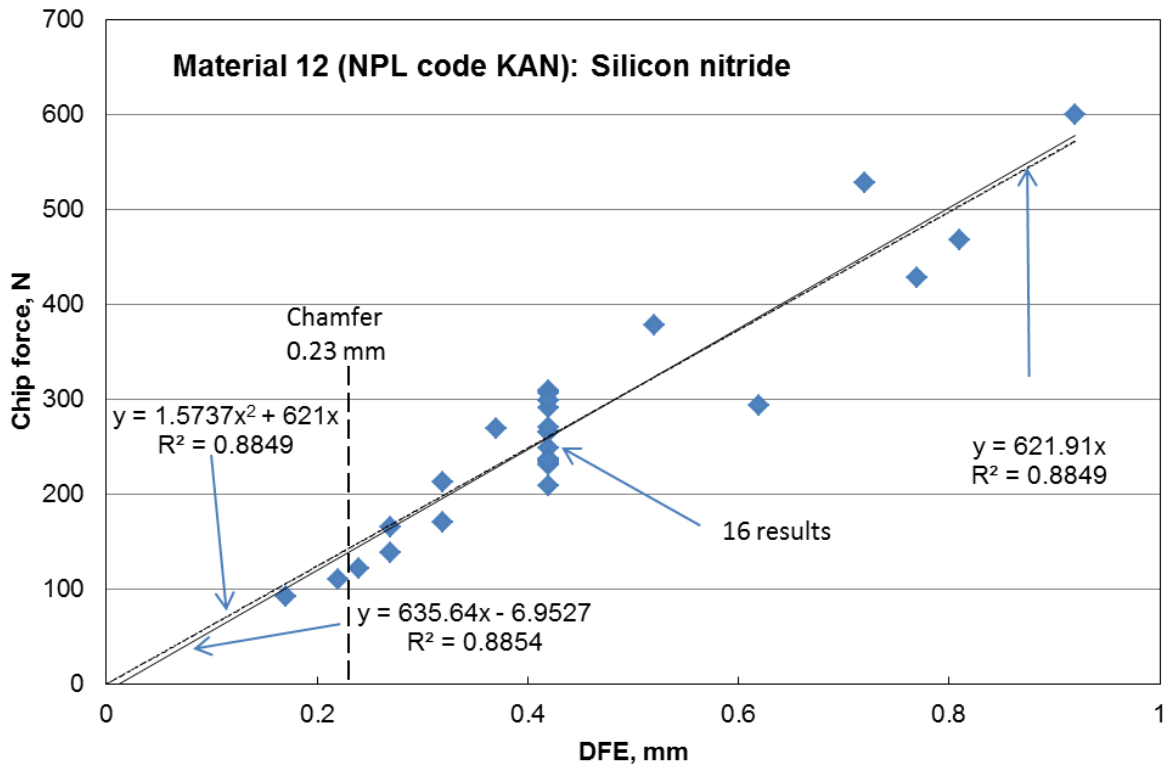
Material 9. Alumina/silicon carbide



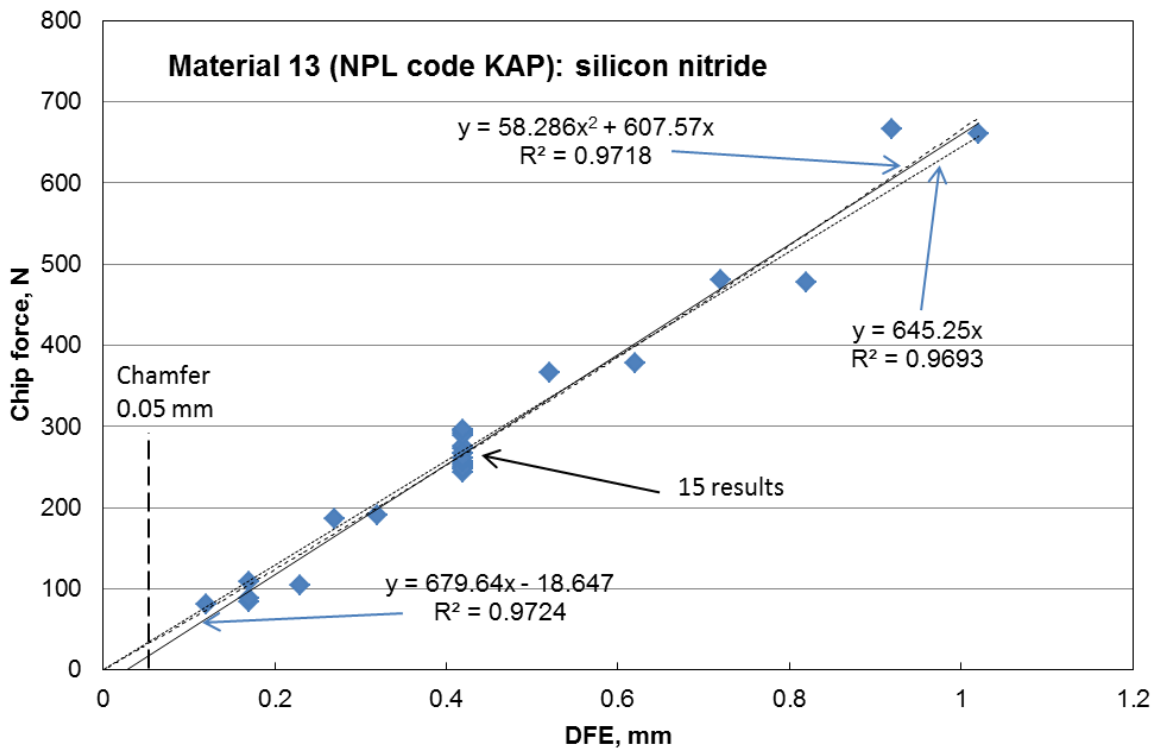
Material 10. Alumina/silicon carbide



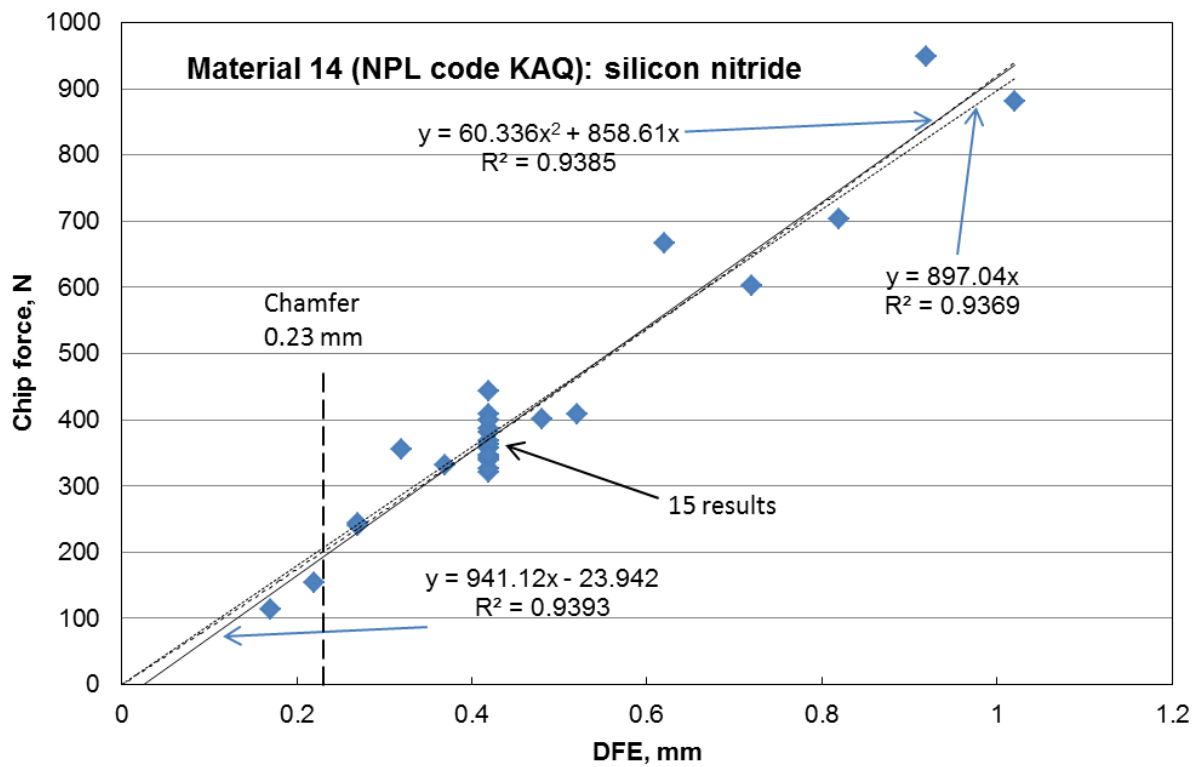
Material 12. Silicon nitride



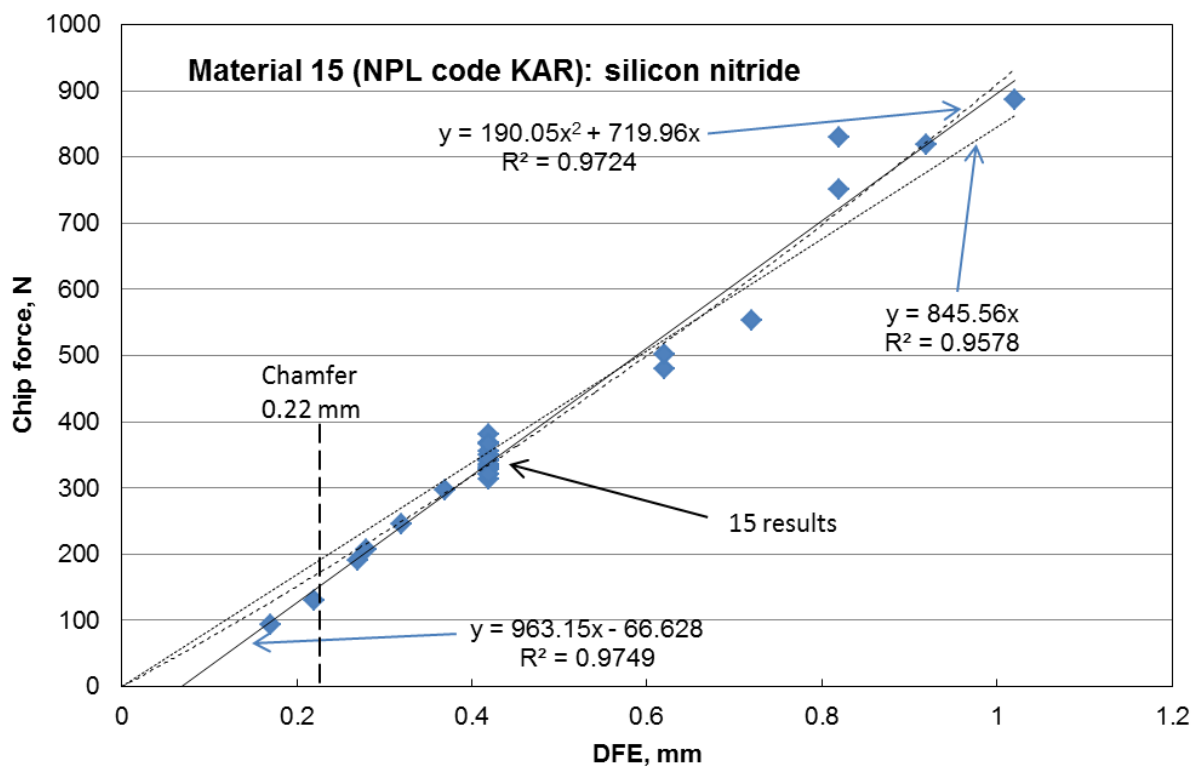
Material 13. Silicon nitride



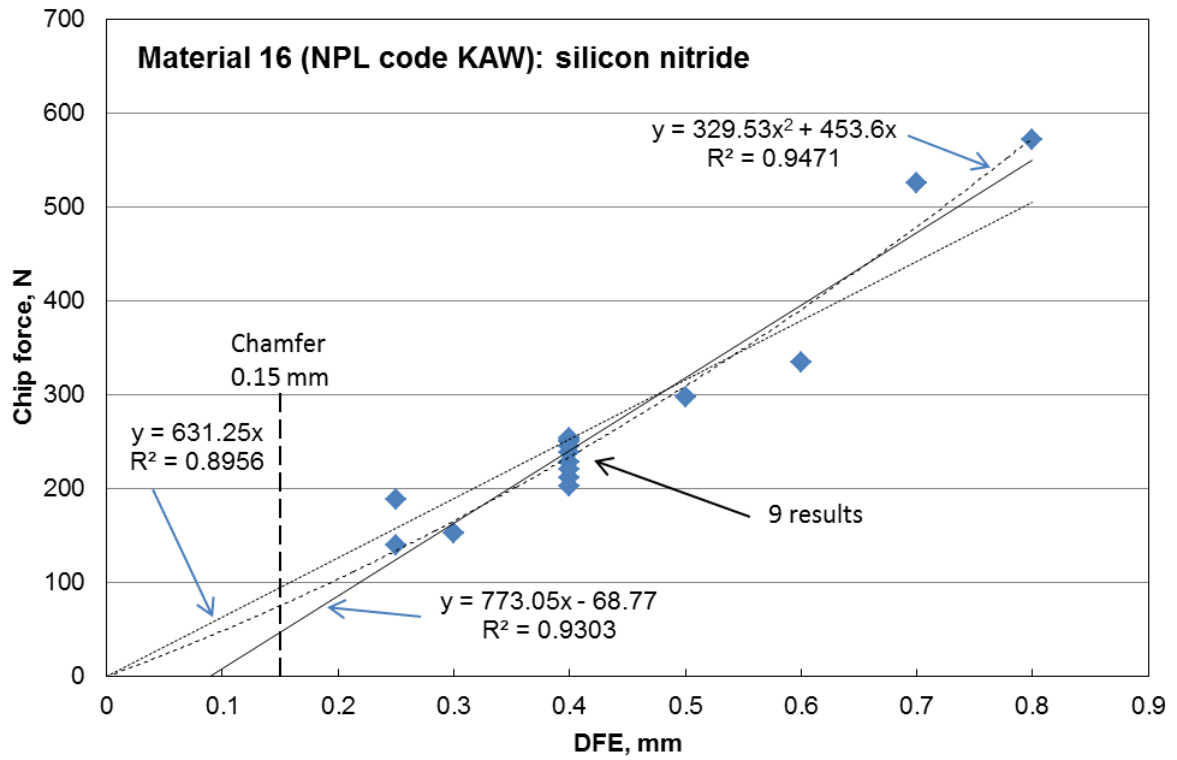
Material 14. Silicon nitride



Material 15. Silicon nitride



Material 16. Silicon nitride



Material 17. Silicon nitride/titanium nitride

